Science of the Total Environment 646 (2019) 19–28

Contents lists available at ScienceDirect

Science of the Total Environment

journal homepage: www.elsevier.com/locate/scitotenv

An integrated approach to identify quantitative sources and hazardous areas of heavy metals in soils

Jianshu Lv [a,b,*], Yang Liu [c]

[a] College of Geography and Environment, Shandong Normal University, Jinan 250014, China
[b] State Key Laboratory of Estuarine and Coastal Research, East China Normal University, Shanghai 200062, China
[c] Business School, University of Jinan, Jinan 25002, China

HIGHLIGHTS

- An integrated approach was proposed to examine sources and hazardous areas of heavy metals.
- FMDM was employed to establish background standards and pollution thresholds.
- PMF with FMDM background was used to partition source contributions.
- SGCS with FMDM pollution thresholds was applied to determine hazardous areas.

GRAPHICAL ABSTRACT

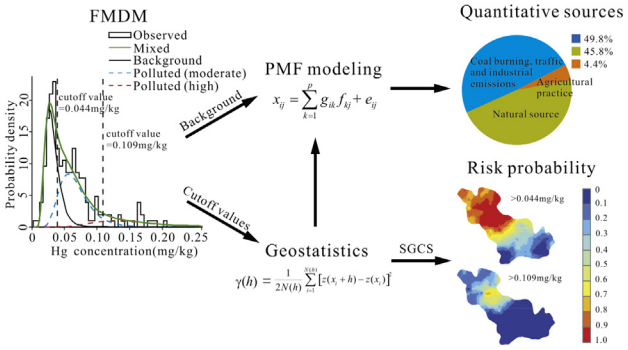

ARTICLE INFO

Article history:
Received 17 May 2018
Received in revised form 17 July 2018
Accepted 18 July 2018
Available online 21 July 2018

Editor: F.M. Tack

Keywords:
Heavy metals
Source
Hazardous areas
Integrated approach
Uncertainty

ABSTRACT

Identifying quantitative sources and hazardous areas of heavy metals is a crucial issue for soil management. For this purpose, an integrated approach composed of finite mixture distribution modeling (FMDM), positive matrix factorization (PMF) and sequential Gaussian co-simulation (SGCS) was proposed. FMDM was used to establish background standards and pollution thresholds. PMF supported by FMDM background standards was applied to estimate the source apportionment. Hazardous areas of single metals were delineated using SGCS with FMDM pollution thresholds and uncertainty analysis, and overall hazardous areas were defined by the presence of multiple metals. This integrated approach was applied to a dataset of seven metals as a case study. FMDM indicated that the distributions of Cr, Cu, Ni, and Zn were fitted to two-dimensional mixture distributions, representing a background distribution and a moderately polluted distribution. The distributions of Cd, Hg, and Pb were composed of a three-component lognormal mixture distribution, corresponding to the background, moderate, and high pollution distributions. Three sources were apportioned. Cr, Cu, Ni, and Zn were dominated by parent materials. Parent materials contributed 52.6%, 45.8%, and 81.9% of Cd, Hg, and Pb concentrations, respectively. Human emissions from coal combustion, industrial work and traffic had significant influences on Hg, Cd, and Pb, with contributions of 49.8%, 26.9%, and 15.6%, respectively. Agricultural practices were exclusively associated with 20.5% of Cd. Overall, hazardous areas exceeding moderate pollution thresholds covered 17.4% of the total area, corresponding to urban areas and industrial sites, whereas overall hazardous areas above high pollution thresholds were limited to 0.01% of the total area.

* Corresponding author at: College of Geography and Environment, Shandong Normal University, Ji'nan 250014, China.
E-mail address: lvjianshu@126.com (J. Lv).

https://doi.org/10.1016/j.scitotenv.2018.07.257
0048-9697/

1. Introduction

Heavy metals are well known because of their ecotoxicity and persistence and are of great importance to soil environments (Alloway, 2013; Rodríguez Martin et al., 2015). Heavy metals in soils are controlled by natural background levels and human inputs with complex influencing mechanisms (Christensen et al., 2018). Natural background levels of heavy metals in soils are mainly inherited from parent rocks. Human activities that influence heavy metal contents include coal combustion, traffic emissions, industrial manufacturing, mining, and agricultural practices(Alloway, 2013), and the impact of anthropogenic inputs commonly exceeds natural background with enhanced urbanization and industrialization. Source apportionment is essential for successfully regulating pollutant inputs, and an adequate understanding of heavy metals background levels facilitates establishing an appropriate standard for soil remediation (Ha et al., 2014; Hu and Cheng, 2013; Li et al., 2015). This combination of natural factors and human activity also results in complex spatial variability (Lv et al., 2013). The areas where heavy metal contents exceed the given thresholds are defined as hazardous areas in this work. Delineating hazardous areas is more valuable for decision-makers for effective soil environment management than mapping spatial variability (Lin et al., 2016).

Receptor models such as absolute principal component score/multiple linear regression (APCS/MLR), positive matrix factorization (PMF), and UNMIX do not depend on prior knowledge of source profiles and have been primarily applied for the identification and apportionment of heavy metal sources (Chen and Lu, 2018; Guan et al., 2018; Perrone et al., 2018; Sofowote et al., 2008). However, the receptor model, as pure multivariate statistical model, may produce biases and uncertainties in the source apportionment. Moreover, the factors from receptor model were identified as different sources by factor loadings of various variables based on the previous knowledge of researchers, which may result in the subjectivity of factor interpretation. The limitations of receptor model could be conducted by comparing the results from multiple models. Finite mixture distribution modeling (FMDM) can build a mixture distribution consisting of several component distributions of heavy metals, and each component represents natural background or human activity distributions (Lin et al., 2010; Portier, 2001; Yang and Chang, 2005). A baseline approach and multivariate analysis are typically used to identify the soil background levels (Albanese et al., 2007; Reimann and de Caritat, 2017; Reimann et al., 2005; Yang and Chang, 2006; Yotova et al., 2018). However, due to current human disturbances of the soil environment, it is difficult to acquire sampling sites that truly represent background soil levels (Yang and Chang, 2006). FMDM can effectively overcome the difficulties associated with defining background sites and has been successfully used to establish background standards and pollution thresholds of heavy metals (Hao et al., 2016; Hu and Cheng, 2013; Lin et al., 2010; Zhi et al., 2016; Zhong et al., 2014). The background standards derived from FMDM can be used to compare to the factor profiles from receptor models; this process facilitates demarcation of the source represented by natural factors and verifies the receptor model results. Zhi et al. (2016) first used FMDM and PMF to apportion the sources of soil Cd in croplands of Eastern China, but PMF failed to obtain a successful source apportionment. In this study, with the support of FMDM, we attempted to apply PMF to estimate source apportionment of heavy metals in soils.

Geostatistical methods including kriging and stochastic simulation provide effective tools to estimate or simulate spatial distributions of heavy metals (Juang et al., 2004; Lv et al., 2013; Rodríguez Martin and Nanos, 2016) and to determine hazardous areas (Chu et al., 2010; Juang and Lee, 1998). Lin et al. (2010), Zhong et al. (2014), and Hao et al. (2016) combined indicator kriging and FMDM to map the spatial patterns of heavy metal pollution in soil. Conditional simulation techniques such as sequential Gaussian simulation (SGS) and sequential indicator simulation (SIS) can be used to avoid the smooth effect of kriged estimation and examine the uncertainty of simulated concentrations (Goovaerts, 1997; Mueller and Ferreira, 2012; Webster and Oliver, 2007). However, conditional simulation requires more random access memory (RAM) and a faster processor than kriging (Emery and Silva, 2009; Yao et al., 2013). With the rapid development of computer hardware, conditional simulation has more potential in environmental studies. The univariate geostatistical simulation tends to ignore spatial interrelation among various variables and may be unsuitable for generating spatial distributions. Multivariate geostatistical simulations with a linear model of coregionalization fitting (LMC) could lead to a better understanding of spatial variability than univariate geostatistical simulation (Boluwade and Madramootoo, 2015; Franco et al., 2006; Liu et al., 2013; Suhrabian and Tercan, 2014). In this study, the spatial probability of pollution was mapped using sequential Gaussian co-simulation (SGCS) with pollution thresholds derived from FMDM, and hazardous areas were determined through minimizing spatial uncertainty.

Together, an integrated approach was proposed to identify quantitative sources and hazardous areas of heavy metals in soils and contains three steps: (1) to explore background standards and pollution thresholds using FMDM, (2) to estimate quantitative source apportionment using PMF supported by FMDM background standards, and (3) to determine hazardous areas using SGCS with the FMDM pollution thresholds and uncertainty analysis. The integrated approach was applied to a heavy metals dataset (Cd, Cr, Cu, Hg, Ni, Pb, and Zn concentrations of 209 surface soil samples) as a case study.

2. Materials and methods

2.1. Sampling and chemical analysis

Boshan, a typical industrial city in eastern China with a total area of 698.2 km^2, was selected as the case study area (Fig. S1). There are three industries in this area, ceramics, coal-fired power, and metal casting; most of this activity is distributed in and around the urban area (Fig. S2). Boshan is one of the most important ceramics production bases in China and contains significant reserves of coal. The intensive industries inevitably result in the accumulation of heavy metals in soils. Furthermore, the rapid industrialization and urbanization in future decades will aggravate this accumulation trend. The elevation ranges from 130 to 1100 m, decreasing in elevation from the south to the north (Fig. S2). The soil parent materials consist of dolomite, limestone, mudstone, sandstone, granite, and hornblendite as well as alluvium and proluvium (Fig. S2).

The study area was divided into 2 km × 2 km cells, and a total of 209 sampling sites were designated at the center of each cell. During field sampling, an alternative location close to predesigned sites was selected to obtain a natural soil in case the soils were unavailable at the original location. The coordinates of the sampling sites were recorded using a hand-held GPS. At each sampling site, four to six subsamples of topsoils (0–20 cm deep) within a 100 m radius were collected and mixed thoroughly in a polyethylene bag. The locations of the sampling sites are indicated in Fig. S1. Soil samples were air-dried and ground to <0.2 mm powder. After digestion of the samples, Cr, Ni, Pb and Zn concentrations were analyzed using a flame atomic absorption spectrophotometer (240 AA Agilent, USA), Cd contents were determined using a graphite furnace atomic absorption spectrophotometer (AA-7000 Shimadzu, Japan), and Hg concentrations were determined with an atomic fluorescence spectrometer (AFS230E Haiguang Analytical Instrument Co., Beijing, China). For details on the measurements, please refer to the related literature (Lu, 2000; Lv et al., 2014; Lv et al., 2013). A standard reference material, GSS-1 soil, obtained from the Center for National Standard Reference Material of China, was used for quality control. The recoveries of all seven metals were 100 ± 10%. Analytical reagent blanks were used in the sample preparation and analytical processes. All measurements were conducted in triplicate, and standard deviations were within ±5% of the mean.

2.2. Methodology

2.2.1. FMDM

The observed concentrations of heavy metals are treated as a mixture distribution model composed of k components (McLachlan and Peel, 2000; Portier, 2001):

$$f(z) = \sum_{i=1}^{k} \pi_i f_i(z) \tag{1}$$

$$\sum_{i=1}^{k} \pi_i = 1, \quad 0 \le \pi_i \le 1, \tag{2}$$

where $f_i(z)$ represents a probability density function of random variables and π_i is the mixed weights of $f_i(z)$ ranging from 0 to 1.

$f_i(z)$ can be any distribution consisting of natural and contamination distributions in heavy metal data. The population of background and contaminated areas would have a right-skewed distribution; thus, the lognormal distribution is commonly recommended in FMDM (Hao et al., 2016; Lin et al., 2010; Zhi et al., 2016). The geometric mean value of background log-normal distributions is the background of heavy metals (Lin et al., 2010; Portier, 2001). In this study, $f_i(z)$ was used as a lognormal distribution.

$$f_i(z|\mu,\sigma^2) = \frac{1}{\sqrt{2\pi}\sigma z} e^{-\frac{(\ln z-\mu)^2}{2\sigma^2}}, \quad z>0 \tag{3}$$

where μ and σ are the mean and standard deviation of $f_i(z|\mu,\sigma^2)$, respectively.

The parameters μ_i, σ_i, and π_i are estimated by using the maximum likelihood method with a combination of a Newton-type algorithm and an EM algorithm.

The hypothesis H_0 is proposed that the estimated model is consistent with the observed distribution, and Chi-square test is used to examine the H_0 (Portier, 2001).

The cutoff values x_0 representing pollution thresholds are determined as follows:

$$\pi_i \int_{x_0}^{+\infty} f_i(z)dz = \pi_{i+1} \int_{-\infty}^{x_0} f_{i+1}(z)dz \tag{4}$$

FMDM was conducted using the Mixdist package (Macdonald and Schwierz, 2018) in the R 3.3.2 software (R Development Core Team).

2.2.2. PMF

PMF is a multivariate factor analysis tool that is used to solve the chemical mass balance model and was utilized using the US-EPA PMF 5.0 program (U.S. Environmental Protection Agency, 2014). The initial data matrix X with the order of $m \times n$ can be expressed as:

$$X = GF + E \tag{5}$$

where G ($m \times p$) is the matrix of the factor contribution, F ($p \times n$) is the matrix of the factor profile, and E ($m \times n$) is the residual error matrix.

E can be written as:

$$e_{ij} = \sum_{k=1}^{p} g_{ik} f_{kj} - x_{ij} \tag{6}$$

where i represents elements from 1 to m, j represents elements from 1 to n, and k represents the source from 1 to p.

Factor contributions and profiles are obtained by minimizing the objective function Q under the constraint of non-negative contributions (Paatero, 1997), which is solved by Multilinear engine-2 (ME-2). The uncertainty is calculated based on the element-specific method detection limit (MDL) and error percent measured by standard reference materials (U.S. Environmental Protection Agency, 2014). In this study, three factors were derived from a run with Q (robust) of 8983.

2.2.3. SGCS

First, Gaussian anamorphosis is used to standardize the original variable into a Gaussian-shaped variable (Lv et al., 2013). LMC fitting is performed on the Gaussian variables. In this study, LMC fitting of seven heavy metals was modeled as the sum of the nugget effect, a spherical structure with a range of 8.2 km, and a Gaussian structure with a range of 42.2 km. The mean error (ME) and the mean of the squared standardized errors (MSSE) calculated from cross validation (Wackernagel, 2003) were close to 0 and 1, ranging from 0.0003 to 0.0007 and 0.981 to 1.195, which suggested that the goodness of fit of the LMC was generally satisfactory.

$$\gamma_{ij}(h) = b_{ij}^0 + b_{ij}^1 \left[\frac{3}{2}\left(\frac{h}{8.2}\right) - \frac{1}{2}\left(\left(\frac{h}{8.2}\right)\right)^3\right] + b_{ij}^2\left(1 - e^{\left(-\frac{h}{42.2}\right)^2}\right) \quad \text{for } 0<h\le 42.2 \text{ km} \tag{7}$$

$$\gamma_{ij}(h) = b_{ij}^0 + b_{ij}^1 + b_{ij}^2 \quad \text{for } h>42.2 \text{ km} \tag{8}$$

where b_{ij}^0 is the nugget effect, b_{ij}^1 is the sill of the spherical structure, and b_{ij}^2 is the sill of the Gaussian structure.

Based on the LMC fitting, the SGCS algorithm can be performed according to Chilès and Delfiner (1999). When the simulation is completed, the simulated normal results are back-transformed to the simulated values in their original units. The SGCS was performed 1000 times to obtain 1000 realizations of seven metals. Spatial distributions of heavy metals were simulated 1000 times by SGCS at the 100 m mesh nodes of a 2D grid, using an optimum number of 10 samples within a neighborhood circle with a 5000 m radius. The single-location uncertainty (Goovaerts, 1997; Juang et al., 2004) and spatial (multi-location) uncertainty (Juang et al., 2004) were used to determine the reliable hazardous areas of single metals exceeding the FMDM thresholds, and the overall hazardous areas of multiple seven metals were defined as the union of hazardous areas for multiple metals. For detailed information, please see the supplementary material. All steps of the SGCS were carried out by using ISATIS 2013 software (Geovariances Inc.).

3. Results

3.1. FMDM fitting of heavy metals

Descriptive statistics for the heavy metal distributions of Boshan were summarized in Table 1. The mean concentrations of Cd, Cr, Cu, Hg, Ni, Pb, and Zn were 0.21, 74.9, 33.4, 0.067, 37.0, 33.6 and 87.3 mg/kg, respectively. All data were positively skewed for seven metals, indicating that there were outliers. The Kolmogorov-Smirnov test suggested that all seven heavy metal concentrations were non-normal. Level II of the Environmental Quality Standard for Soils (EQSS) of China refers to the threshold maintaining agricultural production and human health (State Environmental Protection Administration of China, 1997). Cd appeared to be the most widespread metal exceeding level II of the EQSS with 25 samples (12.0%). There were merely 6, 3, 2, 2, and 1 samples containing Ni, Cr, Hg, Cu, and Zn higher than level II of the EQSS, whereas Pb in all samples was below level II of the EQSS.

The mixture distributions were commonly fitted by a two- and three-component lognormal mixture distribution. The two-component lognormal mixture distribution comprises the background distribution and moderately polluted distribution, whereas the three-component mixture distribution consists of the background distribution mixed with moderate and high pollution distributions. The number of components was determined by examining the characteristics observed

Table 1
Descriptive statistics of heavy metals in soils (n = 209, unit in mg/kg).

	Min	Max	Median	Mean	SD	Skewness	Kurtosis	KS test *P* value	Level II of EQSS
Cd	0.08	1.43	0.20	0.21	0.12	5.709	55.886	0.001	0.3
Cr	22.0	733.5	72.0	74.9	51.06	10.852	135.861	0.000	200
Cu	10.6	117.6	32.0	33.4	12.88	2.449	12.111	0.004	100
Hg	0.010	0.750	0.048	0.067	0.07	5.511	41.635	0.000	0.5
Ni	7.9	568.8	35.5	37.0	37.94	13.364	187.939	0.000	50
Pb	17.8	66.9	31.6	33.6	8.12	1.398	2.605	0.001	300
Zn	43.0	352.1	83.8	87.3	25.21	5.966	58.522	0.000	250

Min: minimum, Max: maximum, SD: standard deviation, KS: Kolmogorov-Smirnov test. EQSS: Environmental Quality Standard for Soils (GB15618-1995).

in the distribution of heavy metals. For example, if the observed distribution has two peaks, it should be fitted with two-dimensional distributions. In this study, the distributions of Cr, Cu, Ni, and Zn were modeled using two-dimension lognormal mixture distributions, and the distributions of Cd, Hg, and Pb were fitted to three-component lognormal mixture distributions (Fig. 1). *P*-values of the fitted mixture modeling of all seven heavy metals were above 0.05, suggesting that these mixture models could accurately describe the observed distributions with the suitable number of components (Table 2).

The geometric mean value of background log-normal distributions of Cd, Cr, Cu, Hg, Ni, Pb, and Zn calculated from FMDM were 0.13, 68.3, 30.9, 0.030, 33.1, 28.8, and 82.6 mg/kg, respectively. The respective cutoff values of moderate pollution for Cd, Cr, Cu, Hg, Pb, and Zn were 0.16, 129.8, 72.2, 0.044, 77.6, 39.2, and 122.4 mg/kg, whereas the respective cutoff values of for Cd, Hg, and Pb high pollution were 0.35, 0.109, and 62.4 mg/kg.

The weight values of the background distribution of Cr, Cu, Ni, and Zn were 0.986, 0.985, 0.991, and 0.954, indicating that these metals mainly originated from natural sources. For Cd and Hg, 64.4% and 42.7% of surface soils suffered from moderate pollution due to human inputs, which were more widespread than the other five metals. The contribution of the background distribution to soil Pb was 83.7% for soils affected by natural sources, but 15.4% of soils with Pb showed moderate pollution due to human activities. For Hg, 12.0% of soils showed high pollution, and the contribution of high pollution distribution to soil Cd and Pb was limited to only 1% and 0.9%. Overall, soil pollution by Cd, Pb, and Hg from anthropogenic sources was more widespread than that by the other four metals.

3.2. PMF modeling of heavy metals

The parameters of PMF modeling with three factors are shown in Table 3. Fig. 2 shows the percentage contribution of three factors, and Fig. S3 indicates the fractional concentrations. The ratios of the predicted to observed values were close to 1, and R^2 varied between 0.71 and 0.93, indicating an accurate fit of the PMF modeling. All heavy metals except Hg had the highest concentration in factor 1. In particular, the Cr, Cu, Ni, and Zn concentrations were exclusively dominated by

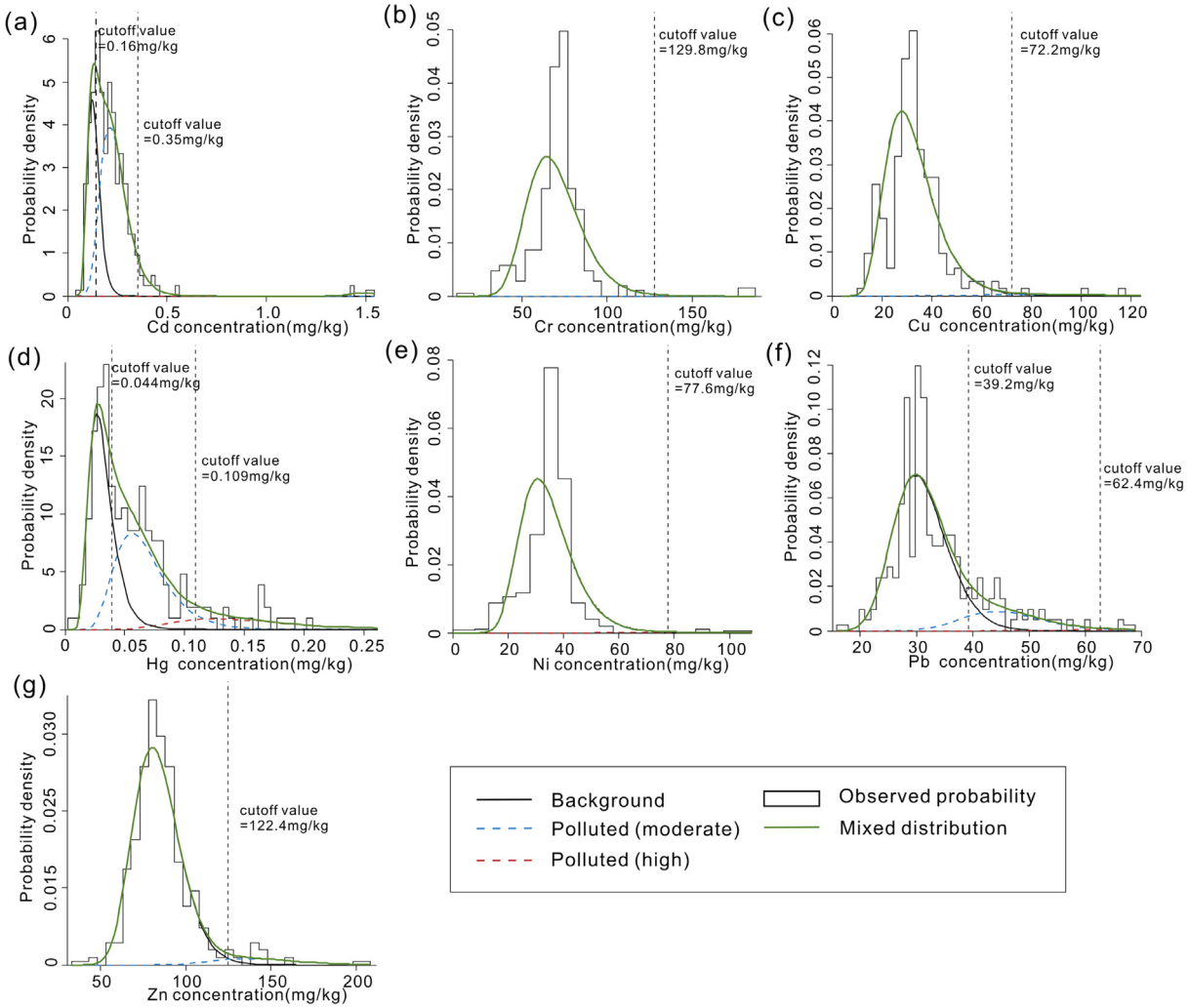

Fig. 1. FMDM fitting of Cd (a), Cr (b), Cu (c), Hg (d), Ni (e), Pb (f), and Zn (g) in soils. Cutoff values (unit in mg/kg), obtained by solving Eq. (4), are indicated in vertical black dot lines.

Table 2
The parameters and the goodness of FMDM fitting and cutoff values.

	Group	Pi	Mu	Sigma	Cutoff	Df	χ^2	*P*-values
Cd	3	0.346	0.13	0.03	0.16	104	103.43	0.50
		0.644	0.24	0.07	0.35			
		0.010	1.49	0.07				
Cr	2	0.986	70.1	16.05	129.8	27	134.34	0.14
		0.014	430.8	98.59				
Cu	2	0.985	32.5	10.57	72.2	33	67.81	0.07
		0.015	94.7	30.84				
Hg	3	0.453	0.032	0.01	0.044	140	63.22	1.00
		0.427	0.067	0.02	0.109			
		0.120	0.151	0.05				
Ni	2	0.991	34.4	9.67	77.6	14	127.02	0.12
		0.009	112.4	31.58				
Pb	3	0.837	31.0	4.91	39.2	44	53.42	0.16
		0.154	46.1	7.30	62.4			
		0.009	66.5	10.53				
Zn	2	0.954	83.7	13.95	122.4	28	36.61	0.13
		0.046	143.6	23.91				

Pi: mixed proportions, Mu: means, Sigma: standard deviations, Df: degrees of freedom, $\chi 2$: Chi-square goodness-of-fit statistic.
If *P*-value is lower than 0.05, reject the hypothesis H_0 that the estimated model is consistent with the observed distribution.

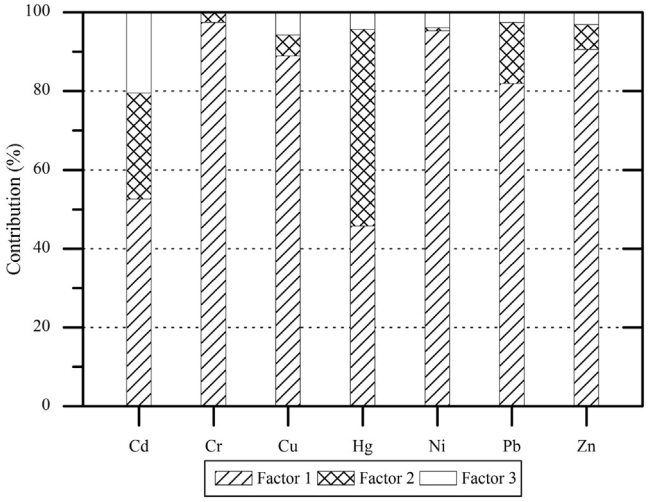

Fig. 2. The source contributions (unit in %) of three factors to seven heavy metals derived from PMF. Factor 1: Natural source, Factor 2: coals combustions, industrial and traffic emissions, Factor 3: agricultural practices.

factor 1, with contributions of 97.4%, 88.9%, 95.3%, and 90.5%. Factor 1 also contributed to 81.9% and 52.6% of the variations in Pb and Cd and was the main sources of these metals. Combined with the results of FMDM, factor 1 can be ascribed to a lithogenic source. Factor 2 contributed 49.8%, 26.9%, and 15.6% of Hg, Cd, and Pb, respectively, and may represent coal combustion, industrial emissions, and traffic emissions due to their widespread occurrence derived from FMDM. Factor 3 was exclusively associated with 20.5% of Cd concentrations, and contributed <6% to the other six heavy metals. Agricultural practice seemed dominate this isolated factor.

3.3. SGCS of heavy metals

Table 4 shows the detailed parameters of LMC fitting. The Gaussian structure was the main component for each heavy metal, followed by the nugget effect and spherical structure. The probabilities of seven metals exceeding moderate and high pollution thresholds are indicated in Fig. 3, and the mean concentrations of seven heavy metals in 1000 realizations are illustrated Fig. S4. The probabilities exceeding moderately polluted cutoffs for Cd, Hg, and Pb showed similar spatial patterns (Fig. 3a, d, and f), and their common hotspots are located at the central part of the study area corresponding to urban areas with a decreasing trend from the center to periphery. Few areas for Cr, Cu, Ni, and Zn were presented in the high probability zone above moderate pollution cutoffs (Fig. 3b, c, e, and g). Hg exhibited some high probability values exceeding high pollution cutoffs (Fig. 3i), but high probability was rarely found for Cd and Pb (Fig. 3h, and j). It is apparent that spatial variations in Cd, Hg, and Pb are affected by human activities.

Spatial uncertainty was used to assess the reliability of the obtained hazardous areas that exceeded pollution thresholds. Table S1 suggests that the joint probability (P_j) increased with the increasing critical probability (P). With the same critical probability, hazardous areas arising from high pollution thresholds tended to have greater joint probability than those from moderate pollution thresholds. The P_j values with moderate pollution thresholds were >0.8 with $P = 0.95$, and the P_j values with high pollution thresholds were >0.85 with $P = 0.95$. Therefore, the critical probability $P = 0.95$ was sufficient to generate the reliable joint probability exceeding moderate pollution and high pollution thresholds and was adopted to determine confidential hazardous areas.

Hazardous areas of heavy metals exceeding FMDM pollution thresholds are indicated in Fig. S5. Approximately 16.4% and 11.5% of the total areas for Cd and Hg were identified as hazardous areas exceeding moderate pollution thresholds, consistent with the urban area and industrial sites (Figs. S5a and d, S2), indicating significant human inputs. <1% of the areas for Cr, Cu, Ni, Pb and Zn were above the moderate pollution thresholds (Fig. S5b, c, e, f, and g). Fig. 4 illustrates the overall hazardous areas of multiple heavy metals. 17.4% of the total areas were classified as overall hazardous areas that exceeded the moderate pollution thresholds (Fig. 4a). The hazardous areas for Cd, Hg, and Pb above high pollution thresholds had areas of 10, 28, and 1 hm^2 and were highly localized, corresponding to individual data points or small groups of points (Fig. S5h, i, and j). In total, an area of 33 hm^2 suffered from hazardous risk resulting from high pollution (Fig. 4b).

4. Discussion

4.1. Comparison of FMDM results with regional background levels and national thresholds

The background of all seven heavy metals derived from FMDM were higher than the corresponding soil background levels of the Shandong Province (0.07 mg/kg for Cd, 64.3 mg/kg for Cr, 22.3 mg/kg for Cu,

Table 3
The validation and results of PMF modeling.

	Model validation				Source profiles (mg/kg)			Source contribution (%)		
	Predicted	Observed	Predicted/observed	R^2	Factor 1	Factor 2	Factor 3	Factor 1	Factor 2	Factor 3
Cd	0.21	0.21	1.00	0.86	0.11	0.06	0.04	52.6	26.9	20.5
Cr	70.0	74.9	0.93	0.71	68.2	1.8	0.0	97.4	2.6	0.0
Cu	34.3	33.4	1.02	0.74	30.5	1.8	2.0	88.9	5.3	5.8
Hg	0.063	0.067	0.95	0.88	0.029	0.032	0.003	45.8	49.8	4.4
Ni	33.8	37.0	0.91	0.85	32.2	0.2	1.3	95.3	0.7	4.0
Pb	33.6	33.6	1.00	0.93	27.5	5.2	0.9	81.9	15.6	2.6
Zn	87.3	87.3	1.00	0.81	79.0	5.5	2.8	90.5	6.3	3.2

Table 4
The parameters of LMC fitting of seven heavy metals.

	Model structure	Nugget	Percentage of Nugget	Sill1	Percentage of Sill1	Sill2	Percentage of Sill2
Cd	Nugget + Sill1 * Sph(8217) + Sill2 * Gau(42208)	0.317	15.6	0.100	4.9	1.612	79.5
Cr	Nugget + Sill1 * Sph(8217) + Sill2 * Gau(42208)	0.389	32.8	0.345	29.1	0.452	38.2
Cu	Nugget + Sill1 * Sph(8217) + Sill2 * Gau(42208)	0.355	22.1	0.190	11.9	1.059	66.0
Hg	Nugget + Sill1 * Sph(8217) + Sill2 * Gau(42208)	0.346	17.7	0.019	1.0	1.586	81.3
Ni	Nugget + Sill1 * Sph(8217) + Sill2 * Gau(42208)	0.436	26.1	0.278	16.7	0.955	57.2
Pb	Nugget + Sill1 * Sph(8217) + Sill2 * Gau(42208)	0.448	26.0	0.339	19.7	0.936	54.3
Zn	Nugget + Sill1 * Sph(8217) + Sill2 * Gau(42208)	0.486	27.0	0.198	11.0	1.115	62.0

Sph: spherical structure, Gau: Gaussian structure.

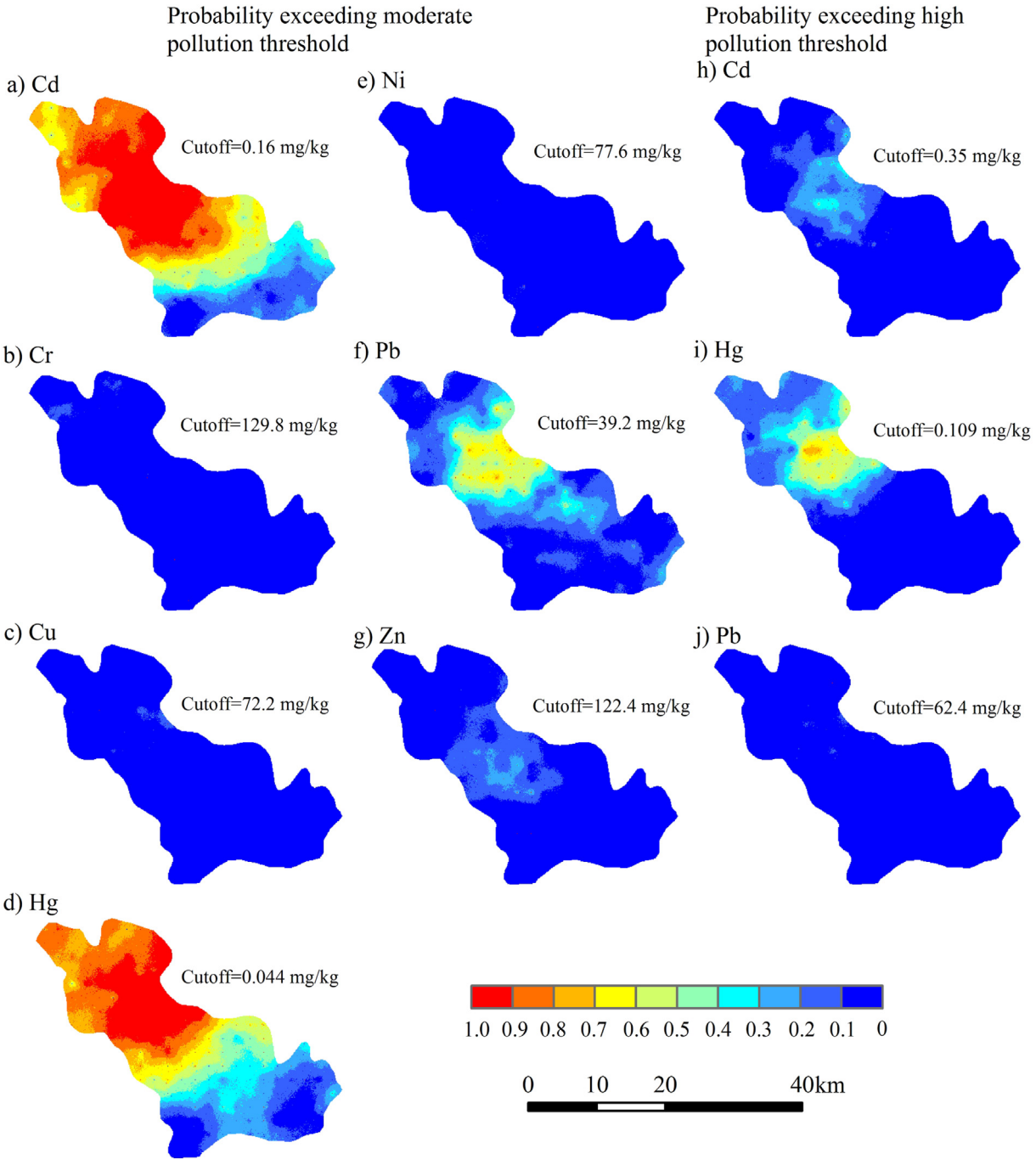

Fig. 3. Probability maps of seven heavy metals exceeding FMDM pollution thresholds. a) Cd, b) Cr, c) Cu, d) Hg, e) Ni, f) Pb, and g) Zn show the probability maps above moderate pollution cutoff, and h) Cd, i) Hg, and j) Pb are the probability maps above high pollution cutoff.

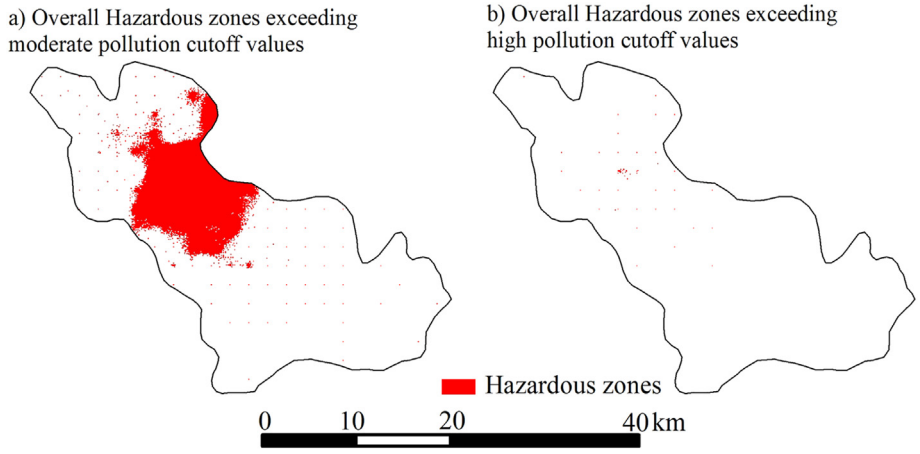

Fig. 4. Overall hazardous areas exceeding the FMDM pollution thresholds. Hazardous areas are indicated in red zones. a) For overall hazardous areas of Cd, Cr, Cu, Hg, Ni, Pb, and Zn above moderate cutoff values. b) For overall hazardous areas of Cd, Hg, and Pb exceeding high pollution cutoffs. (For interpretation of the references to color in this figure legend, the reader is referred to the web version of this article.)

0.016 mg/kg for Hg, 24.4 mg/kg for Ni, 24.5 mg/kg for Pb, and 60.9 mg/kg for Zn) (China National Environmental Monitoring Center, 1990). The high background at Boshan may be attributed to the high percentage of carbonate rocks and mudstone in the parent materials there. Commonly, soils that originate from carbonate rocks and mudstone have higher heavy metals contents than soils that originate from granite, sandstone and alluvium (China National Environmental Monitoring Center, 1990).

The moderately contaminated cutoff values of all seven metals were lower than level II of EQSS. The cutoff values of high pollution for Cd were slightly higher than level II of EQSS, whereas the cutoff values of high pollution for Hg and Pb remained lower than level II of EQSS. It could be suggested that pollution thresholds of Boshan calculated by FMDM were stricter than national thresholds. Level II of EQSS represents the maximum permissible concentration of heavy metals to maintain agricultural production and human health for soils in China. The FMDM cutoffs, calculated from the statistical characteristics of heavy metal concentrations in the study area, could indicate local contamination thresholds. In particular, some regions in developing counties such as Boshan will still experience rapid industrialization and urbanization in future decades, which inevitably leads to the continuous and severe accumulation of heavy metals in soils. The level II of EQSS, as the last line of defense for the soil environment and human health, was 1.5–10 times that of the respective background levels of heavy metals in Boshan. It can be difficult to detect the pollution levels above background using level II of EQSS. Therefore, the thresholds associated with heavy metal pollution assessments should be sensitive and strict in order to regulate the human activities and to prevent the rapid deterioration of the soil environment. Obviously, the FMDM cutoffs could provide earlier warning indicators for soil pollution than the level II of EQSS. Previous studies also compared the FMDM cutoffs with regulation thresholds, and their differences varied locally. Lin et al. (2010) found that the FMDM cut-off values for Cr, Cu and Ni in Chunghua Country, Taiwan were roughly same as the regulatory thresholds. Zhong et al. (2014) reported that the cutoff values for high Cd and As contamination were close to national thresholds, but the cutoff values for high Pb and Hg pollution were less than half of their respective national thresholds. The FMDM cutoff values of As, Cd, Cu, Hg, and Pb in Changchun were found to be less than national thresholds (Hao et al., 2016).

4.2. Source apportionment of heavy metals

4.2.1. Source interpretation of factor 1

Factor 1 produced the dominant contributions of Cr, Cu, Ni, and Zn and significant influences on Cd, Pb, and Hg. The respective contributions of factor 1 to Cd, Cr, Cu, Hg, Ni, Pb, and Zn by PMF were 0.11, 68.2, 30.5, 0.029, 32.2, 27.5, and 79.0 mg/kg (Table 3) and were close to the background standards derived from FMDM (Table 2), indicating that factor 1 represented a strong lithogenic source. Because the concentrations and correlations of heavy metals may vary in different parent materials, the grouping feature derived from PMF could be explained by the mechanism of ionic substitution. For the seven heavy metals in this work, the radii of Cr, Cu, Ni, and Zn are similar, and ionic substitution is commonly observed in minerals (Alloway, 2013; Xu and Tao, 2004). The probability of ionic substitution decreases as radii increase from the aforementioned four metals to Cd, Hg and Pb (Xu and Tao, 2004). In addition, the FMDM illustrated that >95% of soils for Cr, Cu, Ni, and Zn, 83.7% for Pb, 45.3% for Hg, and 34.6% for Cd were below the background distribution. The spatial distributions of Cr, Cu, Ni, and Zn included very small areas with high probability exceeding moderately polluted thresholds, confirming their low human inputs; Cd, Hg, and Pb exhibited some areas with low pollution probabilities (Fig. 3).

Cr and Ni are commonly considered to be the least polluted in China (Jiang et al., 2017; Lv et al., 2015b), and human inputs of these two metals from fertilizers and manure are lower than their background contents in soils (Alloway, 2013). If other metals are classified into a group with Cr and Ni, among the works that use multivariate analysis to analyze the sources of metals, they will be considered to be affected by natural sources (Cai et al., 2015; Liu et al., 2016; Lu et al., 2017; Lv and Yu, 2018; Lv et al., 2013; Nanos and Rodríguez Martin, 2012). Therefore, it could be confirmed that factor 1 indicates natural sources.

4.2.2. Source interpretation of factor 2

Factor 2 was associated with Hg, Cd and Pb. FMDM suggested that these three metals exhibited more widespread pollution than the other four metals. The high probability values of Hg, Cd and Pb that exceeded moderately polluted thresholds corresponded to urban areas with dense industrial factories and traffic lines (Figs. 3, and S2). The anthropic influences on Hg, Cd, and Pb have been clearly demonstrated in previous studies (Franco-Uria et al., 2009; Lv et al., 2013; Lv et al., 2015a). It can be inferred that factor 2 may represent human emissions.

There were three coal-fired power plants with a total capacity of 1000 MW and several coal-fired factories (ceramics and metal casting) in Boshan. The coal-fired power plants and factories were equipped with electrostatic precipitators (ESP) and wet flue gas desulfurization (WFGD). Coal combustion is commonly regarded as the most important source of Hg in China (Wu et al., 2016), with an average Hg concentration of 0.17 mg/kg in coals (Zhang et al., 2012). Most Hg was output to the fluxing gas in the combustion process due to its high volatility

(Vejahati et al., 2010). The species of Hg in fluxing gas are composed of gaseous elementary Hg (Hg^0), gaseous oxidized Hg (Hg^{2+}), and particle-bound Hg. Particle-bound Hg and gaseous Hg^{2+} can be effectively captured by ESP and WFGD, but the water-insoluble Hg^0 is resistant to capture by scrubbers (Srivastava et al., 2006). More than one-half of Hg can escape to the atmosphere after the retaining of scrubbers, and can fall into soils through dry and wet deposition. The removal proportion of Cr, Cd, Ni, Cu, Zn, and Pb by ESP + WFGD was higher than 99% in China (Deng et al., 2014; Zhao et al., 2017). Therefore, it can be concluded that coal combustion contributed a much higher proportion of Hg than other heavy metals.

PbO and CdSSe are widely used as components of pigment in ceramics manufacturing, and Cd and Pb concentrations in ceramics reach 5.27 and 1161 mg/kg (Barros et al., 2007; Lin et al., 2015). The ceramics industry should be responsible for soil Cd and Pb pollution via the emissions of exhaust gas and wastewater. Pb, Cd, and Hg were also related to metal casting factories, and they entered into the soils by atmosphere deposition of fluxing gas, the leaching of industrial residue, and wastewater discharge. Pb could be associated with traffic emissions. Though tetraethyl lead has been banned in China since 2000, the historical Pb emissions from vehicles still exists in the soils there (Lv et al., 2015a).

The local human activities of Boshan contributed much higher proportions of Hg, Cd and Pb than other heavy metals, which are consistent with the results of high loadings of Hg, Cd and Pb, and relatively low loadings of the other four heavy metals in factor 2. The studies by Rodríguez Martín et al. (2006) in the Ebro basin, Lv and Yu (2018) in Gaoqing, Lu et al. (2012) in Shunyi, and Hu et al. (2018) on an alluvial island of the Yangtze River reported that Hg, Cd and Pb were influenced by various human inputs including industrial and traffic emissions and agricultural practices. Consequently, we confirmed that factor 2 was related to coal combustions, industrial emissions, and traffic emissions.

4.2.3. Source interpretation of factor 3

Factor 3 explained 20.5% of Cd concentration and <6% of other metal contents in PMF modeling. Cd is commonly an indicator of the application of chemical fertilizers (Rodríguez Martín et al., 2013), and agricultural practices accounted for 63% of the total annual inventory of Cd in agricultural soils in China (Luo et al., 2009). Farmers must apply excessive chemical fertilizer to maintain and improve soil fertility due to thin soils and serious soil intrusion across most of the study area. The application of chemical fertilizers of Boshan in 2016 was 1210 kg/hm^2, and the respective proportions of compound, nitrate, phosphate, potassium fertilizers were 48.3%, 33.1%, 12.0%, and 6.6%. Cd concentrations of phosphate and compound fertilizers in China are 0.6 and 0.18 mg/kg (Lu et al., 1992), much higher than the background values in the soils of Boshan. The Cd contents in nitrate and potassium fertilizers and Cu, Hg, Pb and Zn in all four fertilizers are much lower than their background values in soils. Therefore, the application of chemical fertilizers could elevate Cd levels more significantly than other metals, which are consistent with the prominent loading of Cd in factor 3. Cai et al. (2015) reported that the group of Cd and As could be defined as an anthropogenic component related to agronomic practices. Zhang et al. (2016) found that Cd was grouped in an isolated group and mainly originated from the application of phosphate fertilizers. Therefore, it can be concluded that factor 3 represented agricultural practices.

4.3. Delineating hazardous areas of heavy metals

SGCS with LMC, involving the spatial relationship of heavy metals in soils, could simulate the spatial distributions of heavy metals in given realizations and to explore spatial uncertainty in their concentrations. Critical probability is crucial for delineating hazardous areas. Previous studies found that critical probabilities of 0.7, 0.9, 0.95, 0.98, and 0.75 could generate a reliable joint probability (Juang et al., 2004; Kerry et al., 2010; Lin et al., 2016; Zhao et al., 2007). In this study, the critical probability with moderate and high pollution thresholds is consistent with Zhao et al. (2007).

The hazardous areas exceeding moderate pollution thresholds were contiguous for Cd and Hg and were localized for Pb, concentrated around urban areas and industrial sites (Figs. S5a, d, f, and S2). Cr, Cu, Ni, and Zn had few hazardous areas above moderate pollution thresholds, which showed no apparent relationship with urban areas and industrial sites and did not reflect significant human inputs (Figs. S5f, and S2). There were no significant hazardous areas for Cd and Pb above the high pollution thresholds (Fig. S5h, j). Only some localized areas of Hg above high pollution thresholds were found, which could be attributed to point pollution from industrial emissions (Fig. S5i). By comparing the single metals and overall hazardous areas, it could be illustrated that the central part of study area was above the moderate pollution thresholds arising from Cd, Hg, and Pb, where several localized areas of high pollution risks dominated by Hg were also revealed. Therefore, it can be concluded that the spatial distributions of Cd, Hg, and Pb are significantly influenced by human activities, and these three heavy metals must be paid more attention. The determination of hazardous areas is similar to previous studies. Zhong et al. (2014) applied indicator kriging to estimate the probabilities of heavy metals exceeding the threshold values calculated from FMDM in a metalliferous industrial district of China and found that Cd, Hg, and Pb were associated with the atmospheric transport and deposition from human emissions. The work of Hao et al. (2016) in Changchun reported that the high probabilities of Cd and Hg exceeding the FMDM cutoff were located in industrial regions and the urban area.

In summary, three sources and hazardous areas of heavy metals were determined by an integrated approach including FMDM, PMF, and SGCS. FMDM offers comparable local background for PMF, avoiding the biases and uncertainties of PMF. SGCS with FMDM pollution thresholds has high sensitivity to detect the hazardous areas of heavy metals, especially that is more meaningful for the regions undergoing rapid industrialization and urbanization. In this study, the results of sources apportionment using FMDM and PMF are consistent, and could verify each other. In addition, hazardous areas delineation for each heavy metal coincides with the sources apportionment. From methodological perspective, the proposed integrated approach proves to be a powerful tool for the source apportionment and hazardous areas delineation of heavy metals in soils, which could provide reliable information for decision-makers for soils management.

5. Conclusions

This study proposes an integrated approach including FMDM, PMF and SGCS to determine quantitative sources and hazardous areas of heavy metals in soils, laying a foundation for soil remediation and effective management recommendations for decision makers. The integrated approach was applied to a heavy metals dataset from Boshan as a case study. Cr, Cu, Ni, and Zn were dominated by parent materials with contributions varying from 88.9% to 97.4%, mainly coming from a natural source. 52.6% of the Cd concentration was controlled by parent materials; coal combustion, industrial emissions, and traffic emissions contributed 26.9% of the Cd concentration, and agricultural practices contributed 20.5% of the Cd concentration. Coal combustion, industrial emissions, and traffic emissions contributed 49.8% of Hg variation, and parent materials contributed 45.8% of Hg variation. 81.9% of Pb was explained by parent materials, whereas coal combustion, industrial emissions, and traffic emissions accounted for 15.6% of Pb concentrations. 17.4% of the total areas were determined as hazardous areas exceeding moderate pollution thresholds, whereas an area of 33 hm^2 suffered from hazardous risk from high pollution. However, as a result of locally relevant metals data, only three sources were identified and apportioned. Further study is needed to apply this integrated approach to apportion more detailed sources of heavy metals.

Conflict of interest

We declared that we have no conflicts of interest to this work.

Acknowledgements

This study was jointly funded by the National Natural Science Foundation of China (41601549, 41701604), the Natural Science Foundation of Shandong Province (ZR2016DQ11), and the Open Research Fund of State Key Laboratory of Estuarine and Coastal Research (SKLEC-KF201710).

Appendix A. Supplementary data

Supplementary data to this article can be found online at https://doi.org/10.1016/j.scitotenv.2018.07.257.

References

Albanese, S., De Vivo, B., Lima, A., Cicchella, D., 2007. Geochemical background and baseline values of toxic elements in stream sediments of Campania region (Italy). J. Geochem. Explor. 93, 21–34.
Alloway, B., 2013. Heavy Metals in Soils. Springer, Dordrecht.
Barros, M.C., Bello, P., Roca, E., Casares, J.J., 2007. Integrated pollution prevention and control for heavy ceramic industry in Galicia (NW Spain). J. Hazard. Mater. 141, 680–692.
Boluwade, A., Madramootoo, C.A., 2015. Geostatistical independent simulation of spatially correlated soil variables. Comput. Geosci. UK 85, 3–15.
Cai, L.M., Xu, Z.C., Bao, P., He, M., Dou, L., Chen, L.G., Zhou, Y.Z., Zhu, Y.G., 2015. Multivariate and geostatistical analyses of the spatial distribution and source of arsenic and heavy metals in the agricultural soils in Shunde, Southeast China. J. Geochem. Explor. 148, 189–195.
Chen, X.D., Lu, X.W., 2018. Contamination characteristics and source apportionment of heavy metals in topsoil from an area in Xi'an city, China. Ecotoxicol. Environ. Saf. 151, 147–154.
Chilès, J.P., Delfiner, P., 1999. Geostatistics: Modelling Spatial Uncertainty. Wiley, New York, USA.
China National Environmental Monitoring Center, 1990. The Background Concentrations of Soil Elements in China. China Environmental Science Press, Beijing.
Christensen, E.R., Steinnes, E., Eggen, O.A., 2018. Anthropogenic and geogenic mass input of trace elements to moss and natural surface soil in Norway. Sci. Total Environ. 613, 371–378.
Chu, H.J., Lin, Y.P., Jang, C.S., Chang, T.K., 2010. Delineating the hazard zone of multiple soil pollutants by multivariate indicator kriging and conditioned Latin hypercube sampling. Geoderma 158, 242–251.
Deng, S., Shi, Y.J., Liu, Y., Zhang, C., Wang, X.F., Cao, Q., Li, S.G., Zhang, F., 2014. Emission characteristics of Cd, Pb and Mn from coal combustion: field study at coal-fired power plants in China. Fuel Process. Technol. 126, 469–475.
Emery, X., Silva, D.A., 2009. Conditional co-simulation of continuous and categorical variables for geostatistical applications. Comput. Geosci. UK 35, 1234–1246.
Franco, C., Soares, A., Delgado, J., 2006. Geostatistical modelling of heavy metal contamination in the topsoil of Guadiamar river margins (S Spain) using a stochastic simulation technique. Geoderma 136, 852–864.
Franco-Uria, A., Lopez-Mateo, C., Roca, E., Fernandez-Marcos, M.L., 2009. Source identification of heavy metals in pastureland by multivariate analysis in NW Spain. J. Hazard. Mater. 165, 1008–1015.
Goovaerts, P., 1997. Geostatistics for Natural Resources Evaluation. Oxford University Press, New York.
Guan, Q.Y., Wang, F.F., Xu, C.Q., Pan, N.H., Lin, J.K., Zhao, R., Yang, Y.Y., Luo, H.P., 2018. Source apportionment of heavy metals in agricultural soil based on PMF: a case study in Hexi Corridor, northwest China. Chemosphere 193, 189–197.
Ha, H., Olson, J.R., Bian, L., Rogerson, P.A., 2014. Analysis of heavy metal sources in soil using kriging interpolation on principal components. Environ. Sci. Technol. 48, 4999–5007.
Hao, L.B., Tian, M., Zhao, X.Y., Zhao, Y.Y., Lu, J.L., Bai, R.J., 2016. Spatial distribution and sources of trace elements in surface soils, Changchun, China: insights from stochastic models and geostatistical analyses. Geoderma 273, 54–63.
Hu, Y.N., Cheng, H.F., 2013. Application of stochastic models in identification and apportionment of heavy metal pollution sources in the surface soils of a large-scale region. Environ. Sci. Technol. 47, 3752–3760.
Hu, W.Y., Wang, H.F., Dong, L.R., Huang, B.A., Borggaard, O.K., Hansen, H.C.B., He, Y., Holm, P.E., 2018. Source identification of heavy metals in peri-urban agricultural soils of southeast China: an integrated approach. Environ. Pollut. 237, 650–661.
Jiang, Y.X., Chao, S.H., Liu, J.W., Yang, Y., Chen, Y.J., Zhang, A.C., Cao, H.B., 2017. Source apportionment and health risk assessment of heavy metals in soil for a township in Jiangsu Province, China. Chemosphere 168, 1658–1668.
Juang, K.W., Lee, D.Y., 1998. Simple indicator kriging for estimating the probability of incorrectly delineating hazardous areas in a contaminated site. Environ. Sci. Technol. 32, 2487–2493.
Juang, K.W., Chen, Y.S., Lee, D.Y., 2004. Using sequential indicator simulation to assess the uncertainty of delineating heavy-metal contaminated soils. Environ. Pollut. 127, 229–238.
Kerry, R., Goovaerts, P., Haining, R.P., Ceccato, V., 2010. Applying geostatistical analysis to crime data: car-related thefts in the Baltic states. Geogr. Anal. 42, 53–77.
Li, Y.B., Duanp, Z.W., Liu, G.L., Kalla, P., Scheidt, D., Cai, Y., 2015. Evaluation of the possible sources and controlling factors of toxic metals/metalloids in the Florida Everglades and their potential risk of exposure. Environ. Sci. Technol. 49, 9714–9723.
Lin, Y.P., Cheng, B.Y., Shyu, G.S., Chang, T.K., 2010. Combining a finite mixture distribution model with indicator kriging to delineate and map the spatial patterns of soil heavy metal pollution in Chunghua County, central Taiwan. Environ. Pollut. 158, 235–244.
Lin, L.Q., Cong, L., Yun, W.H., Yang, J., Ming, H., Wan, Z.B., Kai, C., Lei, H., 2015. Association of soil cadmium contamination with ceramic industry: a case study in a Chinese town. Sci. Total Environ. 514, 26–32.
Lin, W.C., Lin, Y.P., Wang, Y.C., 2016. A decision-making approach for delineating sites which are potentially contaminated by heavy metals via joint simulation. Environ. Pollut. 211, 98–110.
Liu, Y., Lv, J.S., Zhang, B., Bi, J., 2013. Spatial multi-scale variability of soil nutrients in relation to environmental factors in a typical agricultural region, Eastern China. Sci. Total Environ. 450, 108–119.
Liu, Y., Ma, Z.W., Lv, J.S., Bi, J., 2016. Identifying sources and hazardous risks of heavy metals in topsoils of rapidly urbanizing East China. J. Geogr. Sci. 26, 735–749.
Lu, R.K., 2000. Analysis Method of Soil and Agricultural Chemistry. China Agricultural Science & Technology Press, Beijing.
Lu, R.K., Shi, Z.Y., Xiong, L.M., 1992. Cadmium contents of rock phosphates and phosphate fertilizers of China and their effects on ecological environment. Acta Pedol. Sin. 29, 150–157.
Lu, A.X., Wang, J.H., Qin, X.Y., Wang, K.Y., Han, P., Zhang, S.Z., 2012. Multivariate and geostatistical analyses of the spatial distribution and origin of heavy metals in the agricultural soils in Shunyi, Beijing, China. Sci. Total Environ. 425, 66–74.
Lu, J., Li, A.C., Huang, P., 2017. Distribution, sources and contamination assessment of heavy metals in surface sediments of the South Yellow Sea and northern part of the East China Sea. Mar. Pollut. Bull. 124, 470–479.
Luo, L., Ma, Y., Zhang, S., Wei, D., Zhu, Y.G., 2009. An inventory of trace element inputs to agricultural soils in China. J. Environ. Manag. 90, 2524–2530.
Lv, J., Yu, Y., 2018. Source identification and spatial distribution of metals in soils in a typical area of the lower Yellow River, eastern China. Environ. Sci. Pollut. Res. 25, 21106–21117.
Lv, J.S., Liu, Y., Zhang, Z.L., Dai, J.R., 2013. Factorial kriging and stepwise regression approach to identify environmental factors influencing spatial multi-scale variability of heavy metals in soils. J. Hazard. Mater. 261, 387–397.
Lv, J., Liu, Y., Zhang, Z., Dai, B., 2014. Multivariate geostatistical analyses of heavy metals in soils: spatial multi-scale variations in Wulian, Eastern China. Ecotoxicol. Environ. Saf. 107, 140–147.
Lv, J.S., Liu, Y., Zhang, Z.L., Dai, J.R., Dai, B., Zhu, Y.C., 2015a. Identifying the origins and spatial distributions of heavy metals in soils of Ju country (Eastern China) using multivariate and geostatistical approach. J. Soils Sediments 15, 163–178.
Lv, J.S., Liu, Y., Zhang, Z.L., Zhou, R.J., Zhu, Y.C., 2015b. Distinguishing anthropogenic and natural sources of trace elements in soils undergoing recent 10-year rapid urbanization: a case of Donggang, Eastern China. Environ. Sci. Pollut. Res. 22, 10539–10550.
Macdonald, P., Schwierz, C., 2018. R Package Mixdist: finite mixture distribution models. https://cran.r-project.org/web/packages/mixdist/index.html, Accessed date: 17 February 2018.
McLachlan, G., Peel, D., 2000. Finite Mixture Models. Wiley, New York, USA.
Mueller, U.A., Ferreira, J., 2012. The U-WEDGE transformation method for multivariate geostatistical simulation. Math. Geosci. 44, 427–448.
Nanos, N., Rodríguez Martin, J.A., 2012. Multiscale analysis of heavy metal contents in soils: spatial variability in the Duero river basin (Spain). Geoderma 189, 554–562.
Paatero, P., 1997. Least squares formulation of robust non-negative factor analysis. Chemom. Intell. Lab. Syst. 37, 23–35.
Perrone, M.G., Vratolis, S., Georgieva, E., Torok, S., Sega, K., Veleva, B., Osan, J., Beslic, I., Kertesz, Z., Pernigotti, D., Eleftheriadis, K., Belis, C.A., 2018. Sources and geographic origin of particulate matter in urban areas of the Danube macro-region: the cases of Zagreb (Croatia), Budapest (Hungary) and Sofia (Bulgaria). Sci. Total Environ. 619, 1515–1529.
Portier, K.M., 2001. Statistical issues in assessing anthropogenic background for arsenic. Environ. Forensic 2, 155–160.
Reimann, C., de Caritat, P., 2017. Establishing geochemical background variation and threshold values for 59 elements in Australian surface soil. Sci. Total Environ. 578, 633–648.
Reimann, C., Filzmoser, P., Garrett, R.G., 2005. Background and threshold: critical comparison of methods of determination. Sci. Total Environ. 346, 1–16.
Rodríguez Martin, J.A., Nanos, N., 2016. Soil as an archive of coal-fired power plant mercury deposition. J. Hazard. Mater. 308, 131–138.
Rodríguez Martín, J.A., Arias, M.L., Corbi, J.M.G., 2006. Heavy metals contents in agricultural topsoils in the Ebro basin (Spain). Application of the multivariate geoestatistical methods to study spatial variations. Environ. Pollut. 144, 1001–1012.
Rodríguez Martín, J.A., Ramos-Miras, J.J., Boluda, R., Gil, C., 2013. Spatial relations of heavy metals in arable and greenhouse soils of a Mediterranean environment region (Spain). Geoderma 200, 180–188.
Rodríguez Martin, J.A., De Arana, C., Ramos-Miras, J.J., Gil, C., Boluda, R., 2015. Impact of 70 years urban growth associated with heavy metal pollution. Environ. Pollut. 196, 156–163.
Sofowote, U.M., McCarry, B.E., Marvin, C.H., 2008. Source apportionment of PAH in Hamilton Harbour suspended sediments: comparison of two factor analysis methods. Environ. Sci. Technol. 42, 6007–6014.
Srivastava, R.K., Hutson, N., Martin, B., Princiotta, F., Staudt, J., 2006. Control of mercury emissions from coal-fired in electric utility boilers. Environ. Sci. Technol. 40, 1385–1393.

State Environmental Protection Administration of China, 1997. Environmental Quality Standard for Soils (GB15618-1995). Standards Press of China, Beijing.
Suhrabian, B., Tercan, A.E., 2014. Multivariate geostatistical simulation by minimising spatial cross-correlation. Compt. Rendus Geosci. 346, 64–74.
U.S. Environmental Protection Agency, 2014. EPA Positive Matrix Factorization (PMF) 5.0 Fundamentals and User Guide (Washington, DC 20460).
Vejahati, F., Xu, Z., Gupta, R., 2010. Trace elements in coal: associations with coal and minerals and their behavior during coal utilization – a review. Fuel 89, 904–911.
Wackernagel, H., 2003. Multivariate Geostatistics. Springer Verlag, Berlin.
Webster, R., Oliver, M.A., 2007. Geostatistics for Environmental Scientists. Wiley, Chichester.
Wu, Q.R., Wang, S.X., Li, G.L., Liang, S., Lin, C.J., Wang, Y.F., Cai, S.Y., Liu, K.Y., Hao, J.M., 2016. Temporal trend and spatial distribution of speciated atmospheric mercury emissions in China during 1978–2014. Environ. Sci. Technol. 50, 13428–13435.
Xu, S., Tao, S., 2004. Coregionalization analysis of heavy metals in the surface soil of Inner Mongolia. Sci. Total Environ. 320, 73–87.
Yang, S.Y., Chang, W.-L., 2005. Use of finite mixture distribution theory to determine the criteria of cadmium concentrations in Taiwan farmland soils. Soil Sci. 170, 55–62.
Yang, S.Y., Chang, W.-L., 2006. Comparing the classification of copper concentrations in Taiwan farmland soils by baseline method and finite mixture distribution model. J. Chin. Agric. Eng. 52, 23–29.
Yao, R.J., Yang, J.S., Gao, P., Shao, H.B., Chen, X.B., Yu, S.P., 2013. Multivariate simulation and assessment of three dimensional spatial patterns of coastal soil salinity using ancillary variables. Fresenius Environ. Bull. 22, 39–52.
Yotova, G., Padareva, M., Hristova, M., Astel, A., Georgieva, M., Dinev, N., Tsakovski, S., 2018. Establishment of geochemical background and threshold values for 8 potential toxic elements in the Bulgarian soil quality monitoring network. Sci. Total Environ. 643, 1297–1303.
Zhang, L., Wang, S.X., Meng, Y., Hao, J.M., 2012. Influence of mercury and chlorine content of coal on mercury emissions from coal-fired power plants in China. Environ. Sci. Technol. 46, 6385–6392.
Zhang, J.J., Wang, Y., Liu, J.S., Liu, Q., Zhou, Q.H., 2016. Multivariate and geostatistical analyses of the sources and spatial distribution of heavy metals in agricultural soil in Gongzhuling, Northeast China. J. Soils Sediments 16, 634–644.
Zhao, Y.C., Xu, X.H., Huang, B., Sun, W.X., Shao, X.X., Shi, X.Z., Ruan, X.L., 2007. Using robust kriging and sequential Gaussian simulation to delineate the copper- and lead-contaminated areas of a rapidly industrialized city in Yangtze River Delta, China. Environ. Geol. 52, 1423–1433.
Zhao, S.L., Duan, Y.F., Wang, C.P., Liu, M., Lu, J.H., Tan, H.Z., Wang, X.B., Wu, L.T., 2017. Migration behavior of trace elements at a coal-fired power plant with different boiler loads. Energy Fuel 31, 747–754.
Zhi, Y.Y., Li, P., Shi, J.C., Zeng, L.Z., Wu, L.S., 2016. Source identification and apportionment of soil cadmium in cropland of Eastern China: a combined approach of models and geographic information system. J. Soils Sediments 16, 467–475.
Zhong, B.Q., Liang, T., Wang, L.Q., Li, K.X., 2014. Applications of stochastic models and geostatistical analyses to study sources and spatial patterns of soil heavy metals in a metalliferous industrial district of China. Sci. Total Environ. 490, 422–434.